Investigation of Mechanical Properties of Nitrogen-containing Graphene using Molecular Dynamics Simulations

Shingo Okamoto and Akihiko Ito

***Abstract*—We investigated the mechanical properties of nitrogen-containing graphene under tensile loading via molecular dynamics (MD) simulations. In the MD simulation, we used three types of potential functions: the second–generation reactive empirical bond order (REBO) potential for covalent C–C bonds, the Tersoff potential for covalent C–N bonds, and the Lennard–Jones potential for the interlayer interaction of graphite. The effects of nitrogen content and different distributions of nitrogen atoms in graphene on its properties were studied. It was found that a nitrogen content of up to 4% had little effect on the mechanical properties of graphene except when two nitrogen atoms contained in graphene adjoined each other.**

***Index Terms*—graphene, molecular dynamics, nitrogen, tensile strength**

I. Introduction

GLOBAL warming and the exhaustion of fossil fuels have recently attracted worldwide attention. This situation necessitates the development of new technologies that take into account environmental problems. Carbon materials are being investigated as potential candidates for the resolution of these problems owing to their superior mechanical and electrical properties. In particular, graphene and graphite have been found to have excellent strength (~130 GPa) and the same Young's modulus (~1 TPa) as that of diamond. Therefore, more studies have recently been conducted on graphene and graphite [1], [2]. It is crucial to clarify the mechanical properties of graphene and graphite, which are the basic structures in carbon materials, to develop high-performance carbon materials.

In general, carbon materials derived from raw materials contain impurities such as oxygen, nitrogen, or hydrogen atoms, and these impurities may affect the mechanical and electronic properties of the materials. Recently, Shen *et al*. [3], [4] investigated the effects of nitrogen (N) doping on the mechanical properties of ultrananocrystalline diamond (UNCD) films, using molecular dynamics (MD) simulations. They demonstrated that the strength of the N-doped UNCD films decreases with increasing number density of the dopant N atoms. Similarly, nitrogen atoms may also decrease the strength of graphene and graphite. In this study, we investigated the influence of the nitrogen atom on the mechanical properties of graphene under tensile loading, via MD simulations. In addition, we clarified the influence of the different forms of nitrogen distributions in the graphene structure on mechanical properties of graphene.

Manuscript received December 14, 2011. This work was supported in part by the Ring-Ring project of JKA.

Shingo Okamoto is with the Graduate School of Science and Engineering, Ehime University, 3 Bunkyo-cho, Matsuyama 790-8577, Japan (e-mail: okamoto.shingo.mh@ehime-u.ac.jp).

Akihiko Ito is with the Graduate School of Science and Engineering, Ehime University, 3 Bunkyo-cho, Matsuyama 790-8577, Japan. He is also with the Composite Materials Research Laboratories, Toray Industries, Inc., Masaki-cho 791-3193, Japan (e-mail: Akihiko_Ito@nts.toray.co.jp).

II. Method

A. Potential Function

In the present study, we used three types of interatomic potentials: the second-generation reactive empirical bond order (2nd REBO) [5], Tersoff [6], [7], and Lennard–Jones potentials. The 2nd REBO potential for covalent C–C bonds is given by (1):

$$E_{REBO} = \sum_i \sum_{j>i} \left[V_R\left(r_{ij}\right) - B_{ij}^{*} V_A\left(r_{ij}\right) \right]. \tag{1}$$

The terms $V_R(r_{ij})$ and $V_A(r_{ij})$ denote the pair-additive interactions that reflect interatomic repulsions and attractions, respectively. The B_{ij}^{*} denotes the bond-order term.

The Tersoff potential for covalent C–N bonds is given by (2):

$$V = \frac{1}{2} \sum_{i \neq j} \left[f_C\left(r_{ij}\right) A_{ij} \exp\left(-\lambda_{ij} r_{ij}\right) - b_{ij} f_C\left(r_{ij}\right) B_{ij} \exp\left(-\mu_{ij} r_{ij}\right) \right], \tag{2}$$

where the parameter b_{ij} is the bond-order term that depends on the local environment.

$$b_{ij} = \chi_{ij} \left(1 + \beta^{n_i} \zeta_{ij}^{n_i}\right)^{-1/2n_i} \tag{3}$$

$$\zeta_{ij} = \sum_{k \neq i,\, j} f_C\left(r_{ik}\right) g\left(\theta_{ijk}\right) \quad , \tag{4}$$

$$g\left(\theta_{ijk}\right) = 1 + \frac{c_i^2}{d_i^2} - \frac{c_i^2}{d_i^2 + \left(h_i - \cos\theta_{ijk}\right)^2} \ , \tag{5}$$

where θ_{ijk} is the angle between bonds ij and ik.

The parameters A_{ij}, B_{ij}, λ_{ij}, and μ_{ij} depend on the atom type, namely, carbon or nitrogen. For atoms i and j (of different types), these parameters are

$$A_{ij} = \left(A_i \times A_j\right)^{\frac{1}{2}}, \ B_{ij} = \left(B_i \times B_j\right)^{\frac{1}{2}} \tag{6}$$

ISBN: 978-988-19251-1-4
ISSN: 2078-0958 (Print); ISSN: 2078-0966 (Online)

$$\lambda_{ij} = \frac{(\lambda_i + \lambda_j)}{2},\ \mu_{ij} = \frac{(\mu_i + \mu_j)}{2}, \qquad (7)$$

where the parameters with a single index represent the interaction between atoms of the same type.

The parameter χ_{ij} in (3) takes into account the strengthening or weakening of the heteropolar bonds. There is no data for the determination of χ_{ij} for C–N interaction at present. It is impossible to use the data for the determination of χ_{ij} for C–N interaction at present. In our model, this χ_{ij} is set to 0.8833 to obtain the lattice constants a and b of the graphitic-C_3N_4 orthorhombic structure as 4.10 and 4.70Å, respectively. From discussions on the N–N interaction, we know that the N molecule does not interact with other atoms, because of its high binding energy (9.8 eV) and that it diffuses through the crystal and exits the surface. In our model, to keep the nitrogen molecule stable inside the crystalline structure, $\chi_{N\text{-}N}$ is set to zero [3], [7].

The 2nd REBO and Tersoff potentials contain the same cutoff function $f_c(r)$, as given in (8). It is known that for these potential functions, the interatomic force increases dramatically at $r = R_{min}$ and approaches zero at $r = R_{max}$ owing to the discontinuity of the second derivatives of the cutoff function, and this dramatic increase in the interatomic force greatly affects the tensile strength. In this work, the cutoff length R_{min} of both the 2nd REBO and the Tersoff potentials is set to 2.1 Å to avoid the dramatic increase in interatomic forces [8].

$$f_c(r) = \begin{cases} 1, & r < R_{min} \\ \left\{ 1 + \cos\left[\frac{\pi(r - R_{min})}{R_{max} - R_{min}} \right] \right\} / 2, & R_{min} < r < R_{max} \\ 0, & r > R_{max} \end{cases} . \qquad (8)$$

The interatomic force curves of the C–C and C–N bonds of sp^2 structure are shown in Fig. 1. The force of the C–N bond is stronger than that of the C–C bond. The dramatic increase in the force curve disappears gradually.

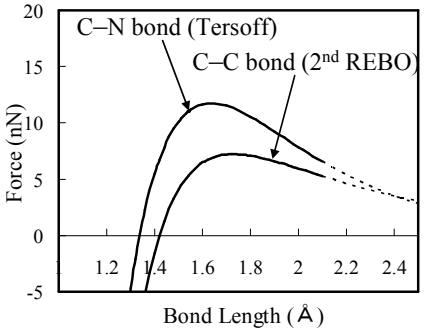

Fig. 1. Interatomic forces of C–C and C–N bonds.

The Lennard–Jones potential for interlayer interaction in the graphitic-C_3N_4 model is given by (9):

$$V^{LJ} = 4\varepsilon \left\{ \left(\frac{r_0}{r_{ij}} \right)^{12} - \left(\frac{r_0}{r_{ij}} \right)^{6} \right\} . \qquad (9)$$

The uses of the 2nd REBO and Lennard–Jones potentials and the Tersoff and Lennard–Jones potentials are switched according to the interatomic distance and bond order [9].

B. *Analysis model*

The crystal structure of orthorhombic graphitic-C_3N_4 [10] is shown in Fig. 2. All the covalent bonds are C–N ones. The unit cell that is enclosed by the box has two lattice constants a and b. The analysis model used in determining the parameter χ_{ij} in the Tersoff potential is shown in Fig. 3. The fundamental cell is composed of six layers of graphitic–C_3N_4 sheets, which are stacked in an AB type sequence. Each layer consists of 48 carbon atoms and 64 nitrogen atoms. Periodic boundary conditions are imposed in all the directions.

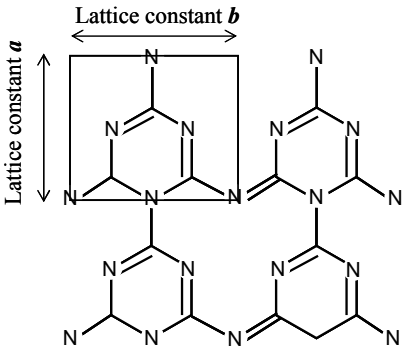

Fig. 2. Orthorhombic structure of graphitic-C_3N_4. (The unit cell is enclosed by the box.)

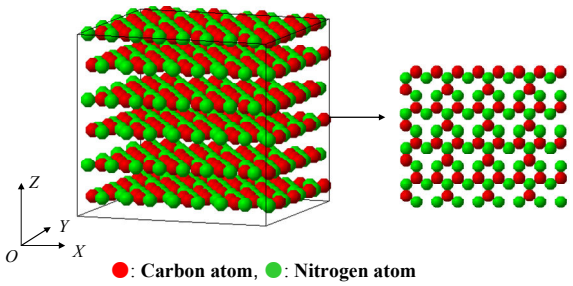

Fig. 3. Configuration of orthorhombic structure of graphitic-C_3N_4 used for determining χ_{ij}.

The analysis models of graphene employed under a condition of zigzag orientation consist of 588 carbon atoms with dimensions identical to those of a real crystallite in typical carbon material, as shown in Fig. 4.

No periodic boundary condition is imposed here to simulate fracture process. The analysis models consist of two parts. One part is referred to as the active zone, in which the atoms move according to their interactions with neighboring atoms. The other part enclosed by the boxes as shown in Fig. 4 is referred to as the boundary zone, in which the atoms are restrained. The thickness l of the boundary zone is $1.5 \times \sqrt{3}a$ for the zigzag tension model, where a is the length of C=C bond of graphene.

The analysis models for uniformly distributed nitrogen atoms in graphene are shown in Fig. 5. The carbon atoms in the active zone of the graphene model, as shown in Fig. 4, are replaced with the N atoms such that the distance between neighboring N atoms is consistently uniform.

ISBN: 978-988-19251-1-4
ISSN: 2078-0958 (Print); ISSN: 2078-0966 (Online)

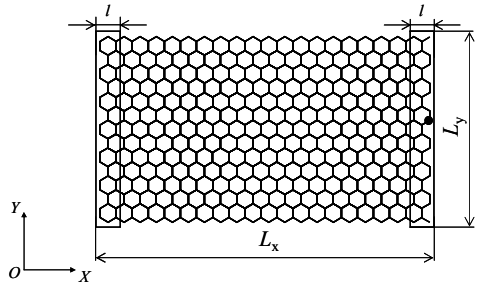

- The atom fixed in the Y direction during an initial relaxation.

Fig. 4. Configuration of graphene used under zigzag tension.

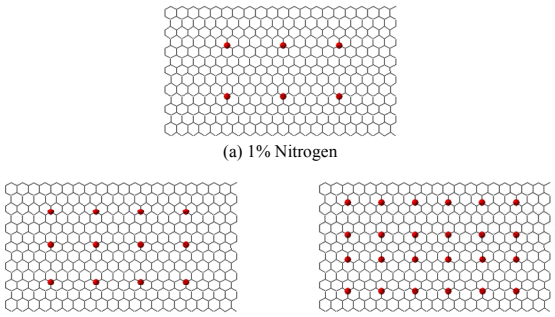

Fig. 5. Analysis models for nitrogen-containing graphene for the different nitrogen contents.

Three cases with differing nitrogen contents, namely, 1%, 2%, and 4%, are investigated.

In the analysis models of randomly distributed N atoms in graphene, random carbon atoms in the active zone are replaced with nitrogen atoms using a pseudorandom number.

C. MD simulation

All the MD calculations employ the velocity Verlet method to calculate the time integral of the equations of motion of atoms. The velocities of all atoms are adjusted simultaneously using the velocity scaling method [11] in order to control the temperature of the object by the preset temperature T_{SET}. The mass of carbon atoms, m_C, and the mass of nitrogen atoms, m_n, are 1.9927×10^{-26} kg and 23.253×10^{-27} kg, respectively. The time step is 1.0 fs.

Determination of the parameter in the Tersoff potential

We determined the parameter $\chi_{\mathrm{C\text{-}N}}$ in the Tersoff potential by calculating the lattice constants of graphitic-C_3N_4 via the MD simulations under a constant pressure and temperature, that is, the NPT ensemble at 1.0×10^{-17} K.

The pressure P_{IJ} and stress σ_{IJ} for the directions X, Y, and Z, given by (10) and (11), are determined by calculating the kinetic energies of and interatomic forces on atoms in the fundamental cell:

$$P_{IJ} = \frac{1}{v}\left(\sum_{i \in v} m\overline{V_I^i V_J^i} + \sum_{i \in v} \overline{I^i F_J^i} \right) \quad (I = X, Y, Z; J = X, Y, Z) \quad (10)$$

$$\sigma_{IJ} = \frac{1}{v}\left(\sum_{i \in v} m\overline{V_I^i V_J^i} + \sum_{i \in v} \overline{I^i F_J^i} \right) - P \quad (I = X, Y, Z; J = X, Y, Z), \quad (11)$$

where v denotes the volume, m is either m_c or m_n, and P denotes the external pressure. The pressure is adjusted by controlling the volume of the fundamental cell using (12) such that the all components of the output stress tensor for graphitic-C_3N_4 are zero:

$$L_I\left(1 + \alpha_I\left(P_{II} - P_{SET}\right)\right) \rightarrow L_I \qquad (I = X, Y, Z), \quad (12)$$

where L_I denotes the length of the fundamental cell in the I direction. P_{SET} is the preset external pressure, and α_I is an appropriate constant. In this study, P_{SET} is set to 1 atm and α_I is set to 0.03.

The initial positions of the atoms are given such that the analysis model becomes identical to the crystal structure of graphitic-C_3N_4. All the atoms are relaxed in unloaded states for 19,000 MD simulation steps. Then, the lattice constants a and b are sampled for 2,000 MD simulation steps and averaged.

Tension of nitrogen-containing graphene

Next, we investigated the mechanical properties of nitrogen-containing graphene by using MD simulations under a constant volume and temperature, that is, the NVT ensemble at 300 K.

The atomic stress acting on each atom is calculated to obtain the stress–strain curves and visualize stress distribution during tensile loadings. The atomic stress $\sigma^i{}_J$ for each of the X, Y, and Z directions of J is obtained by calculating the kinetic energies of atom i, the interatomic force acting on it, and the volume occupied by it, as given in (13).

$$\sigma^i{}_J = \frac{1}{\Omega^i}\left(m\overline{V^i{}_J V^i{}_J} + \overline{J^i F^i{}_J} \right). \qquad (13)$$

Here, Ω^{i} denotes the volume occupied by atom i, which is referred to as the atomic volume. This volume is calculated by averaging the volume of all atoms in the initial structure of each system. m can be either m_{c} or m_{n}. $F^i{}_J$ denotes the interatomic force acting on atom i from the neighboring atoms. The global stress of an analysis model is calculated by averaging over all atoms in each system.

The initial positions of the atoms are given such that the analysis model becomes identical to the crystal structure of N-containing graphene at 300 K. First, the atoms of the analysis model are relaxed until the stresses are stabilized for 10,000–14,000 MD simulation steps. The atoms in the active zone are relaxed in all the directions. The atom shown by a black circle is relaxed in only the X direction. The atoms in the left-hand side boundary zone are relaxed in only the Y direction. The atoms in the right-hand side boundary zone except the atom shown by a black circle are relaxed in only the X and Y directions. After the atoms are relaxed, constant displacements are applied to the atoms in the boundary zones to simulate uniaxial tensile loading in the X direction. The atoms in the boundary zones are restrained in the X and Z directions. The atoms in the active zone of the analysis model and those in the boundary zones are relaxed for all the directions and only the Y direction, respectively for 7,000 MD simulation steps. The strain increment $\Delta\varepsilon$ is 0.004. The Young's moduli are obtained from the slopes of the straight lines in the range, where the relation between the stress and strain is linear, and tensile strengths are given by the peak of

ISBN: 978-988-19251-1-4
ISSN: 2078-0958 (Print); ISSN: 2078-0966 (Online)

the nominal stress–nominal strain curves.

III. Results and Discussion

A. Determination of the parameter in the Tersoff potential

The lattice constants a and b with the parameter $\chi_{C\text{-}N}$ are shown in Fig. 6. The relations between both the lattice constants a and b and $\chi_{C\text{-}N}$ are found to be linear for $\chi_{C\text{-}N}$ from 0.8 to 1.0. $\chi_{C\text{-}N}$ was determined to be 0.8833 when a and b were 4.10 and 4.70Å, respectively, on the basis of the work of Alves *et al*. [10].

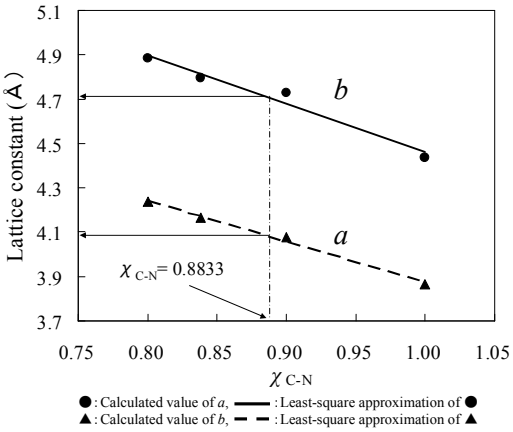

Fig. 6. Lattice constants a and b as a function of parameter $\chi_{C\text{-}N}$.

B. Mechanical properties of nitrogen-containing graphene

Examples of the stress-strain curves of graphene containing uniformly distributed nitrogen atoms are shown in Fig. 7. The calculated tensile strengths and Young's moduli are listed in Table I.

The increase in stress is delayed for the nitrogen-containing graphene. This delay is attributed to the nitrogen atoms that prevent flatness of the graphene sheet. It is found that the tensile strength and Young's modulus of the graphene sheet do not change much with a change in the nitrogen content.

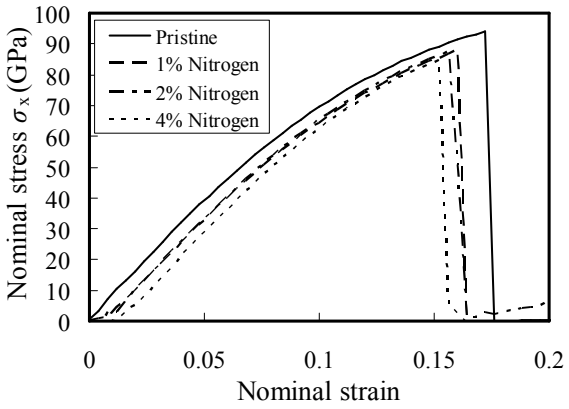

Fig. 7. Stress-strain curves of graphene containing uniformly distributed nitrogen atoms.

TABLE I
Mechanical Properties of Graphene Containing Uniformly Distributed Nitrogen Atoms

Nitrogen content (%)	Tensile strength (GPa)	Young's modulus (GPa)
0	94	786
1	88	758
2	87	774
4	84	772

Snapshots taken during the tensile loadings are shown in Fig. 8. In all the cases, fractures occur because of cleavage of the C–C bond, which is in proximity to a C–N bond.

Examples of the stress-strain curves of graphene containing randomly distributed nitrogen atoms are shown in Fig. 9. The calculated tensile strengths and Young's moduli are listed in Table II. The decrease in the tensile strengths and fracture strain is found to be larger than that in the tensile strengths and fracture strain in graphene containing uniformly distributed nitrogen atoms. In particular, the decrease in the tensile strength is largest for graphene with a nitrogen content of 2%. The Young's modulus does not change much with a change in the nitrogen content.

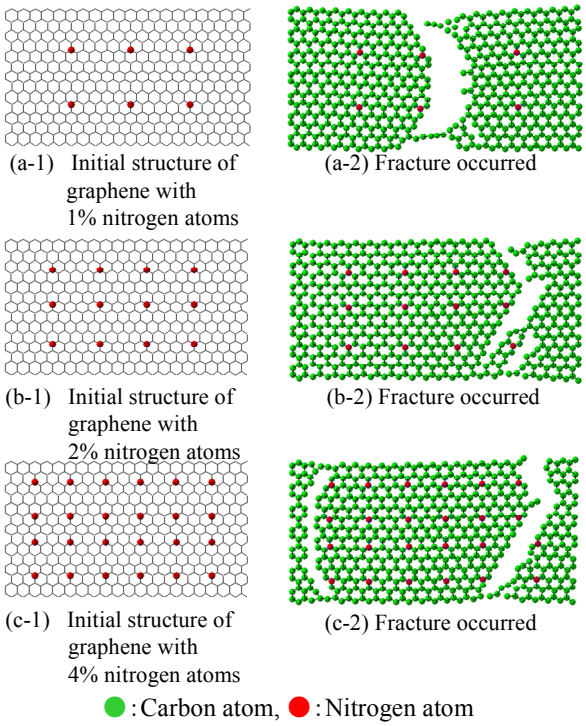

Fig. 8. Structures before tensile loading and after fracture for graphene containing uniformly distributed nitrogen atoms.

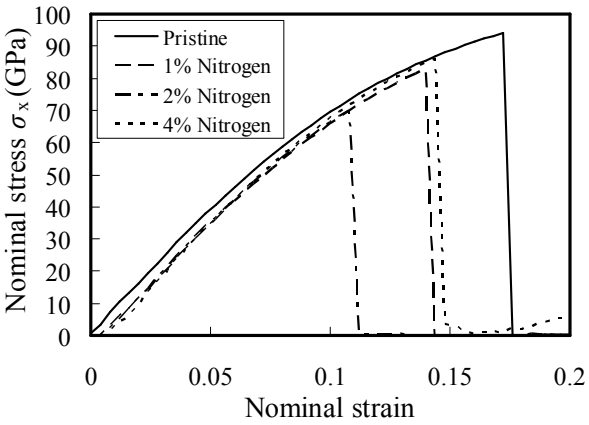

Fig. 9. Stress-strain curves of graphene containing randomly distributed nitrogen atoms.

ISBN: 978-988-19251-1-4
ISSN: 2078-0958 (Print); ISSN: 2078-0966 (Online)

TABLE II
MECHANICAL PROPERTIES OF GRAPHENE CONTAINING RANDOMLY DISTRIBUTED NITROGEN ATOMS

Nitrogen content (%)	Tensile strength (GPa)	Young's modulus (GPa)
0	94	786
1	82	766
2	70	809
4	86	840

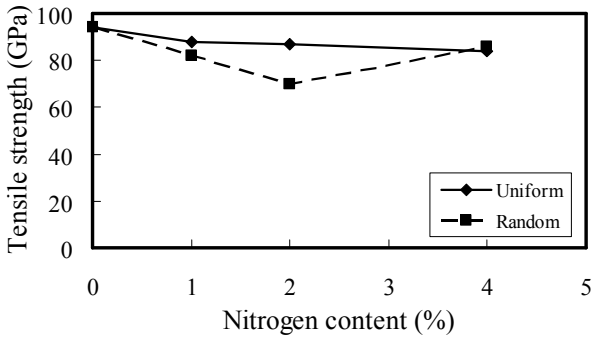

Fig. 10. Tensile strengths as a function of content of uniformly or randomly distributed nitrogen atoms.

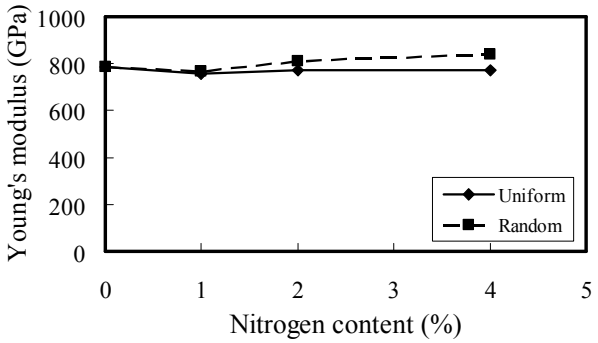

Fig. 11. Young's moduli as a function of content of uniformly or randomly distributed nitrogen atoms.

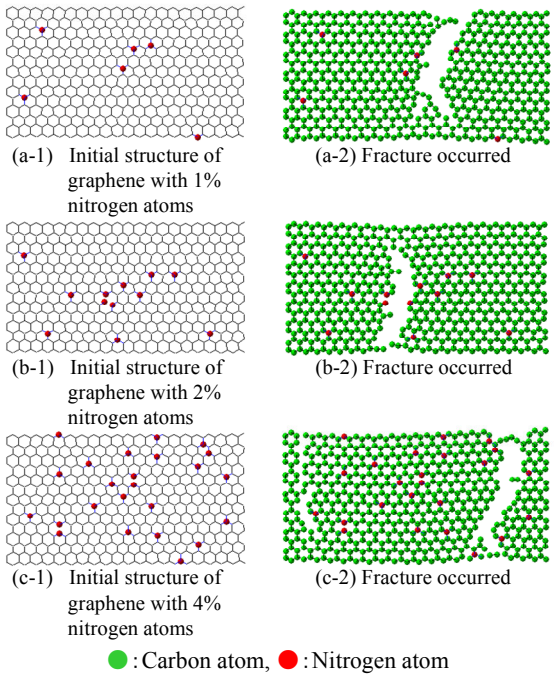

Fig. 12. Structures before tensile loading and after fracture for graphene containing randomly distributed nitrogen atoms.

The relation between the tensile strength and the nitrogen content is shown in Fig. 10. The difference in the tensile strengths between the uniform and random distributions is largest for the sheet with a 2% nitrogen content. However, little difference is observed in nitrogen-containing graphene with other contents of 1% and 4%. The relation between the Young's modulus and the nitrogen content is shown in Fig. 11. For both the uniform and random distributions of nitrogen atoms, the Young's modulus barely changes with changing nitrogen content.

We examined the atomistic structures under tensile loadings in order to determine the decrease in tensile strength for graphene containing 2% nitrogen atoms that are randomly distributed. Snapshots taken during the tensile loadings are shown in Fig. 12. In the case of the 2% nitrogen content ((b-1) and (b-2)), fracture occurs at the point where two nitrogen atoms adjoin each other. Although graphene with the 4% nitrogen content also contains adjoining nitrogen atoms, fracture occurs by starting from the other point. The difference between these fracture modes for 2% and 4% nitrogen atoms contents is attributed to whether the two nitrogen atoms adjoining each other are located perpendicular to the tensile axis. The uniaxial loading does not affect the separation of two neighboring nitrogen atoms when they are perpendicular to the tensile axis.

C. Influence of distance between two nitrogen atoms on tensile strength of graphene

Examples of the stress-strain curves of graphene containing two nitrogen atoms that are located at an interval *d* are shown in Fig. 13. The calculated tensile strengths and Young's moduli are listed in Table III.

It is found that the tensile strength decreases with decreasing distance between two nitrogen atoms. The decrease in the tensile strength in the case of pristine graphene is about 25%

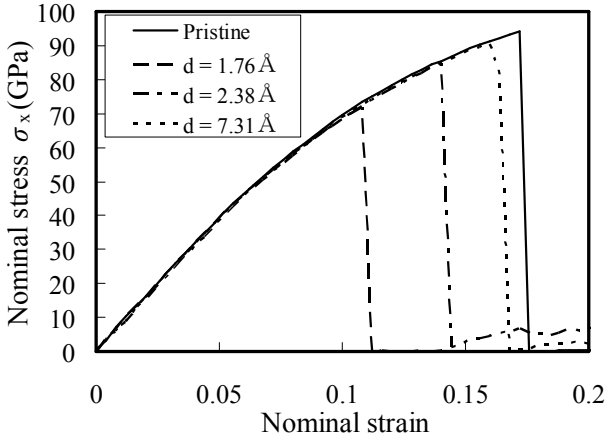

Fig. 13. Stress-strain curves of graphene containing two nitrogen atoms located at an interval *d*.

TABLE III
MECHANICAL PROPERTIES OF GRAPHENE CONTAINING TWO NITROGEN ATOMS

d (Å)	Tensile strength (GPa)
1.76	71
2.38	84
7.31	90

ISBN: 978-988-19251-1-4
ISSN: 2078-0958 (Print); ISSN: 2078-0966 (Online)

when two nitrogen atoms adjoin each other, i.e., when *d* is 1.76Å.

The relation of the tensile strengths with the distance between two nitrogen atoms is shown in Fig. 14. The larger the distance of separation between two nitrogen atoms, the higher is the tensile strength. This relation is almost constant when *d* is over 2.38Å. When *d* between two nitrogen atoms is 1.76Å, the strength agrees with that for graphene containing 2% nitrogen atoms that are randomly distributed.

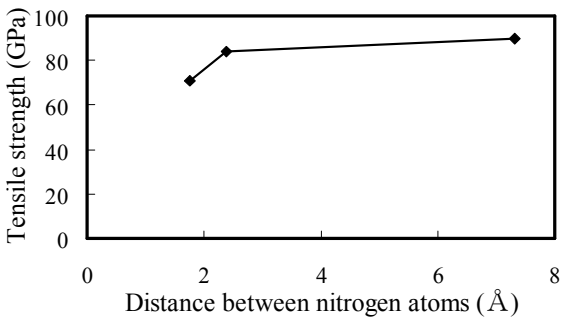

Fig. 14. Relation of tensile strength with the distance between two nitrogen atoms.

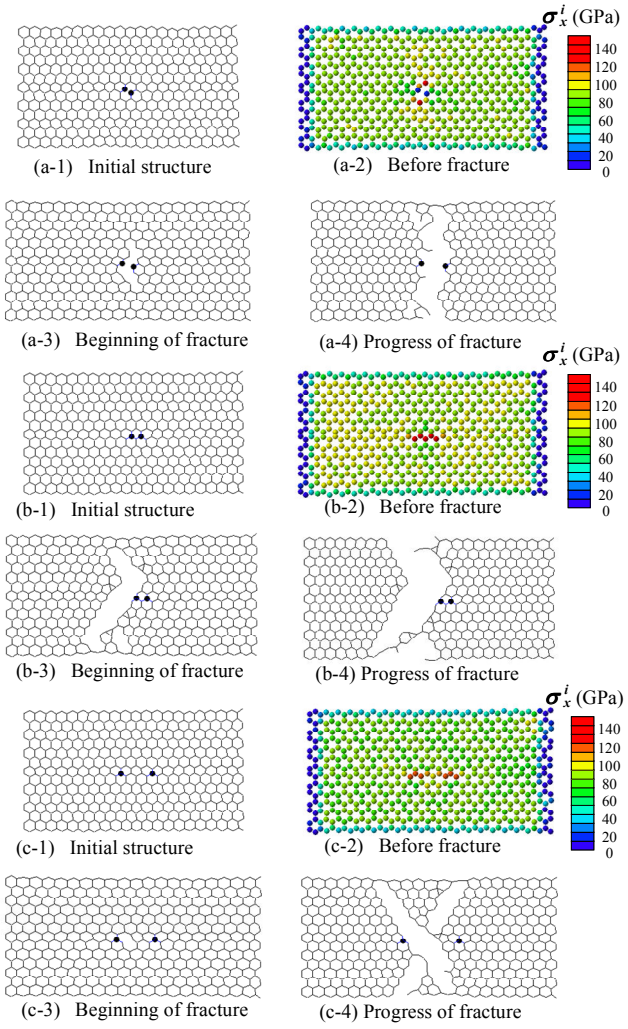

Fig. 15. Stages of fracture progress in graphene containing two nitrogen atoms at different intervals *d*: 1.76 Å ((a-1)–(a-4)), 2.38Å ((b-1)–(b-4)), and 7.31Å ((c-1)–(c-4)).

When two nitrogen atoms are located alternately in the form of N–C–N, i.e., when *d* is 2.38Å, the strength agrees with that for graphene containing 1% and 4% nitrogen atoms that are randomly distributed.

Snapshots taken during the tensile loadings are shown in Fig. 15. In the case of *d* = 1.76Å ((a-1)–(a-4)), fracture occurs at the point where two nitrogen atoms adjoin each other, similar to the case of graphene containing 2% randomly distributed nitrogen atoms (Fig. 12(b-1) and (b-2)). Stress does not concentrate on nitrogen atoms before fracture (a-2). Instead, stress concentrates on the two carbon atoms located alternately after each nitrogen atom. In the case of *d* = 2.38 and 7.31 Å ((b-1)–(b-4) and (c-1)–(c-4), respectively), the stress concentrates on the nitrogen atom and its neighboring carbon atoms. Fracture starts at the cleavage of the C–C bond adjoining the nitrogen atom and not at a C–N bond, because of the stronger binding force of the C–N bond.

IV. Conclusion

We performed MD simulations for tensile loadings of graphene containing nitrogen atoms in order to investigate the effect of the nitrogen atom on the mechanical properties of graphene. As a result, we found that both the strength and the Young's modulus do not change much for a nitrogen content of up to 4%, unless two nitrogen atoms present in graphene adjoin each other. We demonstrated that the difference in the distribution of nitrogen atoms in graphene affects the tensile strength considerably.

References

[1] R. Granatab, V. B. Shenoy, and R. S. Ruoff, "Anomalous strength characteristics of tilt grain boundaries in graphene," *Science*, vol. 330, pp. 946–948, Nov., 2010.

[2] J. R. Xiao, J. Staniszewski, and J. W. Gillespie, Jr., "Tensile behaviors of graphene sheets and carbon nanotubes with multiple Stone-Wales defects," *Mater. Sci. Eng. A*, vol. 527, pp. 715–723, Jan., 2010.

[3] L. Shen and Z. Chen, "An investigation of grain size and nitrogen-doping effects on the mechanical properties of ultrananocrystalline diamond films," *Int. J. Sol. Struct.*, vol. 44, pp. 3379–3392, May, 2007.

[4] L. Shen and Z. Chen, "A study of mechanical properties of pure and nitrogen-doped ultrananocrystalline diamond films under various loading conditions," *Int. J. Sol. Struct.*, vol. 46, pp. 811–823, Feb., 2009.

[5] D. W. Brenner, O. A. Shenderova, J. A. Harrison, S. J. Stuart, B. Ni, and S. B. Sinnott, "A second-generation reactive empirical bond order (REBO) potential energy expression for hydrocarbons," *J. Phys.: Condens. Matter*, vol. 14, pp. 783–802, Jan., 2002.

[6] J. Tersoff, "Modeling solid-state chemistry: interatomic potentials for multicomponent systems," *Phys. Rev. B*, vol. 39, no. 8, pp.5566–5568, Mar., 1989.

[7] J. Tersoff, "Structural properties of amorphous silicon nitride," *Phys. Rev. B*, vol. 58, no. 13, pp. 8323–8328, Oct., 1998.

[8] O. A. Shenderova, D. W. Brenner, A. Omeltchenko, X. Su, L. H. Yang, and M. Young, "Atomistic modeling of the fracture of polycrystalline diamond," *Phys. Rev. B*, vol. 61, no. 6, pp. 3877–3888, Feb., 2000.

[9] S. J. Stuart, A. B. Tutein, and J. A. Harrison, "A reactive potential for hydrocarbons with intermolecular interactions," *J. Chem. Phys.*, vol. 112, no. 14, pp. 6472–6486, Jan., 2000.

[10] I. Alves, G. Demazeau, B. Tanguy, and F. Weill, "On a new model of the graphitic form of C_3N_4," *Solid State Commun.*, vol. 109, pp. 697–701, Mar., 1999.

[11] L. V. Woodcock, "Isothermal molecular dynamics calculations for liquid salts," *Chem. Phys. Lett.*, vol. 10, pp. 257–261, Aug., 1971.

ISBN: 978-988-19251-1-4
ISSN: 2078-0958 (Print); ISSN: 2078-0966 (Online)